A comparison of semi-empirical density functional theories for nucleation

1997 J. Phys.: Condens. Matter 9 L19

(http://iopscience.iop.org/0953-8984/9/3/001)

J. Phys.: Condens. Matter **9** (1997) L19–L26. Printed in the UK PII: S0953-8984(97)79118-5

LETTER TO THE EDITOR

A comparison of semi-empirical density functional theories for nucleation

J C Barrett

Department of Nuclear Science and Technology, Royal Naval College, Greenwich, London SE10 9NN, UK

Received 31 October 1996, in final form 18 November 1996

Abstract. Density gradient theory with two different forms for the equation of state is used to model nonane nucleation. At each temperature considered, the two parameters in the equations of state are found by equating the equilibrium chemical potential and pressure in the liquid and vapour state. The coefficient of the square gradient is then chosen so that the surface tension for a planar surface calculated by density gradient theory matches the experimental value. Results for nucleation rates are compared with density functional calculations following the procedure described by Nyquist *et al* (Nyquist R M, Talanquer V and Oxtoby D W 1995 *J. Chem. Phys.* **103** 1175). The density gradient values are within a factor of ten of the classical theory results and exhibit almost identical temperature dependences. In contrast, the density functional theory predicts rates that are much larger and exhibit weaker temperature dependence than classical theory. The two equations of state predict values that differ by a factor of about ten, indicating that the form of the equation of state in the unstable region is important in determining the nucleation rate from density functional theories. This conclusion is supported by calculations using a model equation of state, for which the chemical potential is three intersecting straight lines.

Density functional theory provides a means of relating thermodynamic properties of inhomogeneous systems to intermolecular potentials without calculating the full partition function. It has been applied to nucleation by Oxtoby and co-workers [1, 2]. Recently Nyquist *et al* [3] have developed a semi-empirical form of density functional theory and compared its predictions with experimental measurements for a number of substances. Previously, Barrett [4] adopted a similar approach for nonane nucleation, but using the simpler density gradient theory together with the empirical Peng–Robinson equation of state [5]. In this letter we compare the predictions of density gradient theory with those of density functional theory in a semi-empirical approach to nonane nucleation. We also compare values using the van der Waals equation of state with those using the Peng–Robinson equation. Finally, we examine the sensitivity of density gradient results to the form of the equation of state in the experimentally inaccessible unstable region between the two spinodals in an analytically soluble model.

In classical nucleation theory, the rate of droplet formation per unit volume for a vapour at temperature T can be expressed as $J_{Cl} = J_0 \exp(-\Delta\Omega_{Cl}/kT)$ where $J_0 = N_{Av}(n_v^2/n_l)\sqrt{(2\sigma/\pi m_v)}$ and the classical change in the grand potential on formation of the critical nucleus is

$$\Delta\Omega_{Cl} = \frac{16\pi\sigma^3}{3(\Delta p)^2} \tag{1}$$

0953-8984/97/030019+08$19.50

where n_v and n_l are the molar densities in the vapour and liquid, N_{Av} is Avogadro's number, σ is the bulk surface tension, m_v is the molecule mass and Δp is the pressure difference between the centre of the droplet and the bulk vapour. Assuming incompressible liquid and ideal gas, this is given by

$$\Delta p = n_l R_G T \ln S \tag{2}$$

where the saturation $S = p_v/p_{ve}$ is the ratio of the vapour pressure to its value at equilibrium, and $R_G = kN_{Av}$ is the gas constant. Note that we are using the historical expression for J_{Cl}, omitting a factor $1/S$ which more careful considerations show should be included [6].

In density functional theories of nucleation [1], $\Delta\Omega$ is given by the value of a functional of the density, n, at the saddle point (i.e. where $\delta\,\Delta\Omega/\delta n = 0$). In its simplest form, known as density gradient theory or the square-gradient approximation, the change in grand potential is given by

$$\Delta\Omega = \int \left(\frac{c}{2}(\nabla n)^2 + [f(n) - \mu(n_v)n] + p_v \right) \mathrm{d}^3\boldsymbol{r} \tag{3}$$

where $f(n)$ is the free energy and $\mu(n)$ the chemical potential (both per unit volume) of a uniform fluid at molar density n. The parameter c can be related to the direct correlation function of the uniform vapour at density n [7] and so is density dependent; however, here we ignore this density dependence. The variational equation $\delta\,\Delta\Omega/\delta n = 0$ for a spherically symmetric droplet profile is then

$$c\,\frac{\mathrm{d}^2 n}{\mathrm{d}r^2} + \frac{2c}{r}\,\frac{\mathrm{d}n}{\mathrm{d}r} = \mu(n) - \mu(n_v). \tag{4}$$

In the planar case, the second term on the left-hand side is missing and n_v has its equilibrium value n_{ve} where $\mu(n_{ve}) = \mu(n_l)$. It is then possible to obtain the surface tension without first calculating the density profile [8]:

$$\sigma = \sqrt{2c} \int_{n_l}^{n_v e} \mathrm{d}n\ [(f(n) - \mu(n_{ve})n) + p_{ve})]^{1/2}. \tag{5}$$

To use these formulae we need expressions for the thermodynamic properties of the uniform fluid at all densities. These can be obtained from the equation of state for the fluid $p \equiv p(n, T)$ using the thermodynamic relations $p = \mu n - f$ and $\mathrm{d}f/\mathrm{d}n = \mu$. In this work, we consider two equations of state: the van der Waals equation, with the Carnahan–Starling form for the three-dimensional hard-sphere repulsive term [9]:

$$p = nR_G T \frac{1 + \eta + \eta^2 - \eta^3}{(1-\eta)^3} - \frac{1}{2}\alpha n^2 \tag{6}$$

and the Peng–Robinson equation [5]:

$$p = \frac{nR_G T}{1 - nb} - \frac{n^2 a}{1 - nb(2 - nb)}. \tag{7}$$

In equation (6), $\eta = n\pi d^3/6$ where d is the hard-sphere diameter. Our choice of equation (7) was influenced by the work of Carey *et al* [8] who used it in a semi-empirical treatment of the surface tension of n-alkanes. Equations (6) and (7) each contain two parameters (α and d in equation (6), a and b in equation (7)). Rather than relate these to microscopic and/or critical properties of the fluid, we choose them so that, at each temperature considered, the pressure and chemical potential of the equilibrium liquid and vapour are equal, i.e. $p(n_{ve}) = p(n_l) = p_{ve}$ and $\mu(n_{ve}) = \mu(n_l)$ where p_{ve} and n_l are the experimentally determined equilibrium vapour pressure and liquid density. Finally the

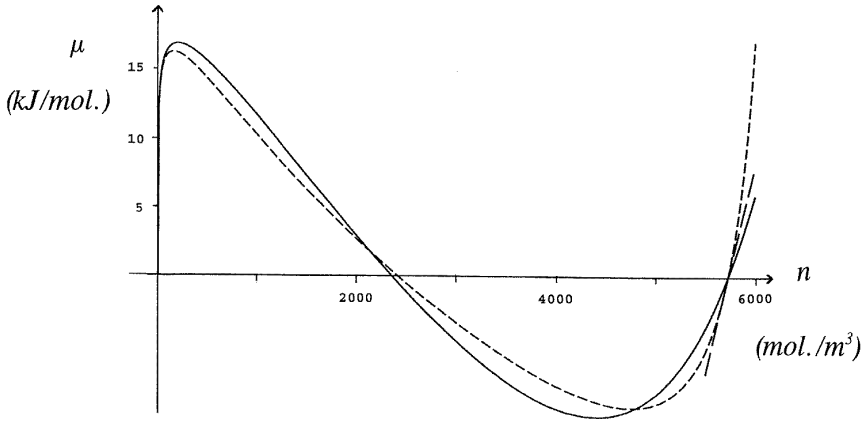

Figure 1. The variation of the chemical potential for van der Waals fluid (solid line) and Peng–Robinson fluid (dashed line). The parameters are chosen to match the equilibrium properties of nonane at 273 K.

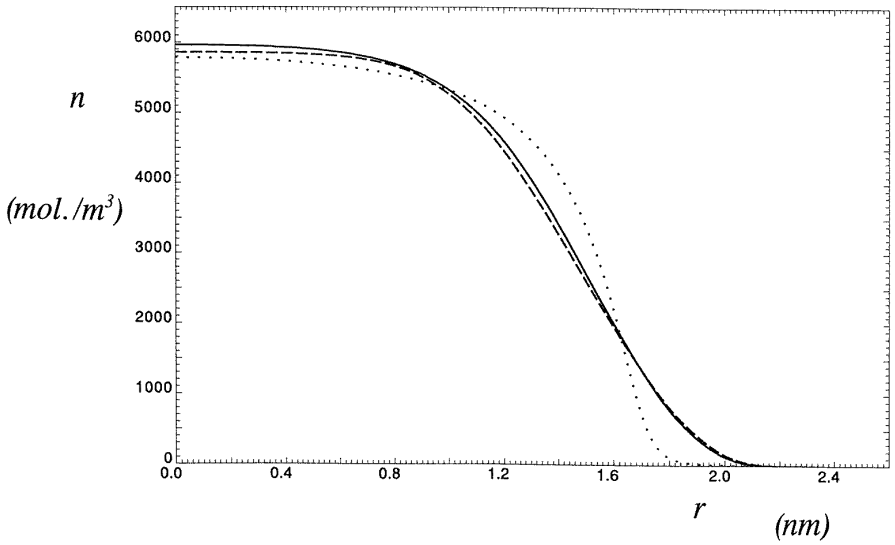

Figure 2. The density profile for nonane at $T = 273$ K, $S = 13.2$. Square-gradient theory results obtained using the van der Waals equation (solid line) and the Peng–Robinson equation (dashed line) Also shown (dotted line) is the profile from the density functional approach of Nyquist *et al* [3].

parameter c is determined at each temperature from the requirement that the surface tension calculated from equation (5) is equal to the experimentally measured value.

We now report the results of some calculations for nonane. The equilibrium thermophysical data needed (equilibrium vapour pressure, bulk liquid density and surface tension) were taken from Hung *et al* [10]. Since α (or a) appears linearly in equation (6) (or (7)) we can eliminate it using the equality of pressures and chemical potentials in liquid and vapour at equilibrium to obtain a single non-linear equation for d (or b). This equation was then

solved by Newton–Raphson iteration. Note that it is necessary to re-evaluate n_{ve} from the condition $p(n_{ve}) = p_{ve}$ at each iteration. Figure 1 shows the chemical potentials resulting from this procedure at $T = 273$ K. Also shown is the straight line through n_l with gradient $1/n_l^2\chi_T$ (where χ_T is the isothermal compressibility of the liquid) which, according to a standard thermodynamic relation, is equal to $\mathrm{d}\mu/\mathrm{d}n$ at n_l. We note that the gradient of μ from the empirical Peng–Robinson equation is closer to this experimental value of $\mathrm{d}\mu/\mathrm{d}n$ than that from the van der Waals equation.

The parameter c was found from equation (5), the integral being evaluated by quadrature, and the differential equation (4) was solved numerically subject to the boundary conditions $\mathrm{d}n/\mathrm{d}r = 0$ at $r = 0$ and $n = n_v$ at $r = r_{max}$ where r_{max} was taken to be twice the classical critical radius. Typical density profiles are shown in figure 2. Also shown is the density profile calculated using the mean-field density functional theory of Oxtoby and Evans [1], as applied to nonane by Nyquist *et al* [3]. In this, the intermolecular potential is divided into a hard-sphere repulsive part and an attractive part, taken to have the Yukawa form. For a uniform fluid, the grand potential in this approach reduces to $-pV$, where p is the van der Waals pressure given by equation (6) (where α is the integrated strength of the attractive part of the potential). Finally, the range parameter in the Yukawa potential is chosen so that the surface tension calculated in this model equals the experimentally measured value. All approaches yield the same values for bulk parameters, and therefore also the same values for classical nucleation rates. However, it can be seen from figure 2 that the profile from density functional theory is much sharper than those from density gradient theory. This is in agreement with the results of Lu *et al* [11] who found that the '10–90' widths of profiles from density gradient theory were larger than those from density functional theories at temperatures far below the critical temperature T_c (using the parameters at $T = 273$ K in the van der Waals equation gives $T_c = 804$ K, significantly higher than the experimental value of 595 K).

Table 1. Temperatures and saturation ratios used in the calculations for figure 3.

T	S	J_{Cl}
233	40.7	2.31
248	25.1	114
258	19.1	2010
273	13.2	8.99×10^4
285	10.0	6.60×10^5
299	7.5	5.78×10^6
315	5.9	1.36×10^9

Once the density profile is known, $\Delta\Omega$ can be found from equation (3) by quadrature. We consider values of $\exp([\Delta\Omega_{cl} - \Delta\Omega]/kT)$ which is equal to the ratio of non-classical to classical nucleation rates, if the prefactor is assumed to be the same in both cases [3]. We find that this ratio varies very weakly with saturation (increasing by a factor of less than 10 as the nucleation rate increases from 1 m^{-3} s^{-1} to 10^{12} m^{-3} s^{-1}) showing that the density gradient approach gives essentially the same saturation dependence as classical theory, as well as experiment and the density functional results of Nyquist *et al* [3]. We have also investigated the ratio of nucleation rates at various temperatures and saturations, as shown in table 1. The temperatures were selected from those at which measurements were made by Hung *et al* [10] and the saturations correspond approximately to an experimentally observed nucleation rate of 10^5 m^{-3} s^{-1}. Figure 3 shows the ratios $J/J_{Cl} = \exp([\Delta\Omega_{cl} - \Delta\Omega]/kT)$

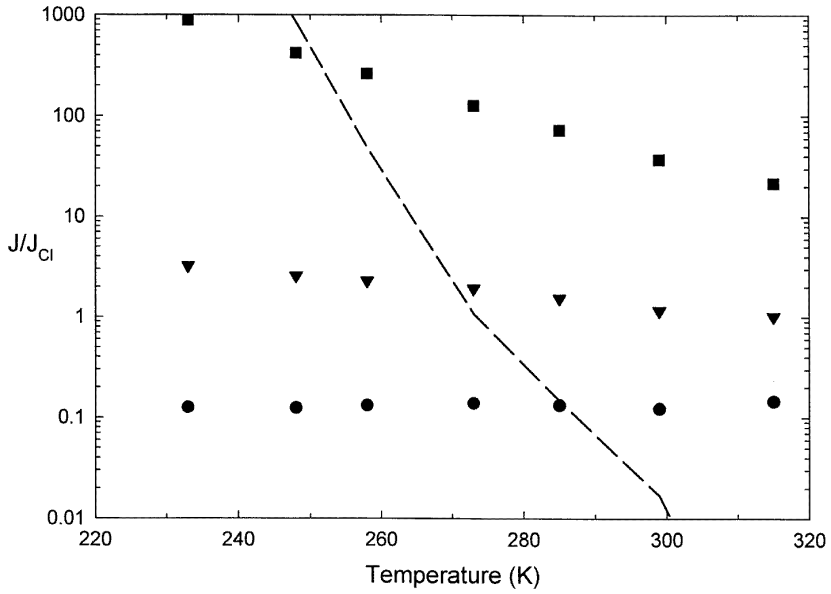

Figure 3. The variation of the ratio J/J_{cl} of the density functional results to classical values using square-gradient theory with the van der Waals equation (circles), the Peng–Robinson equation (triangles) and the non-local functional of Nyquist *et al* (squares). The dashed line indicates the trend of the experimental measurements of Hung *et al* (see the text).

for the three density functional theories considered. Density gradient theory with the van der Waals equation of state gives nucleation rates about one tenth of those of classical theory, but exhibiting almost identical temperature dependence. Using the Peng–Robinson equation of state we obtain rates within a factor of three of classical values with the ratio J/J_{Cl} decreasing slightly with increasing temperature. By contrast, rates from the mean-field density functional theory are significantly larger than classical rates and the ratio J/J_{Cl} exhibits a strong temperature dependence (the density functional nucleation rates do not increase as rapidly with temperature as classical theory rates). The dashed line in figure 3 is $10^5/J_{Cl}$ and so indicates the ratio of experimentally measured rates to classical theory.

Two differences with previously published results should be mentioned: our density functional results are slightly larger than the values of Nyquist *et al* [3], presumably because their values are averages over a number of saturations whereas ours are for a single saturation at each temperature. Our density gradient results using the Peng–Robinson equation differ slightly from those we reported previously [4] since our earlier results were for a constant classical nucleation rate of 10^6 m^{-3} s^{-1} and also used a cruder parametrization of the equation of state.

To investigate further the dependence of nucleation rates in density gradient theory on the form of the equation of state we consider a model system with a chemical potential that varies as shown in figure 4. The chemical potential rises linearly with gradient λ_v^2 as the density increases from n_{ve} to some density n_a, then it falls linearly with gradient $-\lambda_2^2$ as the density increases from n_a to n_b, and finally it rises linearly with density from n_b to n_l (and beyond). The free energy in this model consists of three parabolae, with pairs intersecting at n_a and n_b. It is therefore a straightforward extension of the double-parabola model considered by Iwamatsu [12]. By adjusting λ_2 while keeping λ_v and λ_l constant, we

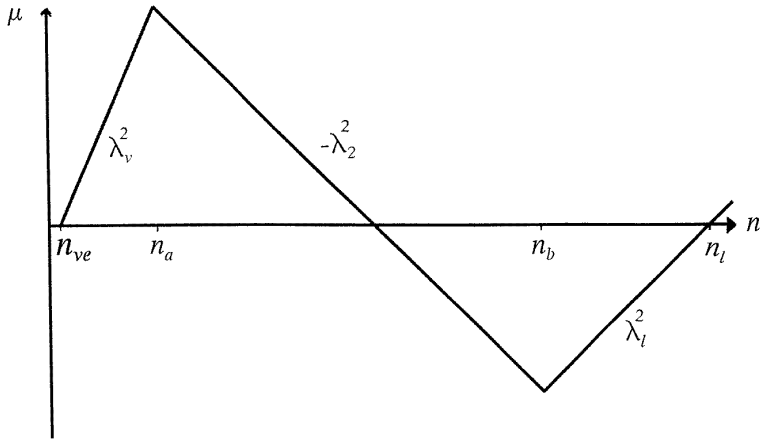

Figure 4. The chemical potential μ as a function of the molar density n for the model fluid.

can investigate the sensitivity of the nucleation rate to the form of the unstable part of the equation of state.

As before, we are interested in comparing the grand potential difference for a droplet from density gradient theory, $\Delta\Omega$, with that from classical theory, $\Delta\Omega_{Cl}$, using a surface tension calculated from density gradient theory. We consider the fractional difference $(\Delta\Omega - \Delta\Omega_{Cl})/\Delta\Omega_{Cl}$ and scale all densities according to $n \to (n - n_{ve})/n_l$. It is then possible to reduce the dependence of the fractional difference to three parameters which we take to be the (scaled) supersaturated vapour density, n_v, and the two ratios λ_l/λ_v and λ_2/λ_v. The equality of the chemical potential and pressure at $n = 0$ and $n = 1$ leads to the following equations relating n_a and n_b to these ratios:

$$\lambda_v^2 n_a - \lambda_2^2(n_b - n_a) + \lambda_l^2(1 - n_b) = 0 \tag{8}$$

$$\lambda_v^2 n_a n_b = \lambda_l^2(1 - n_a)(1 - n_b). \tag{9}$$

Once $\mu(n)$ (and therefore also $f(n)$) is specified, the surface tension in the square-gradient approximation can be found directly from equation (5). In the supersaturated vapour, the classical free-energy change on cluster formation is still found from equation (1), but with Δp now given by

$$\Delta p = \lambda_v^2 n_v + \frac{1}{2}\lambda_v^2 n_v^2\left[\left(\frac{\lambda_v}{\lambda_l}\right)^2 - 1\right]. \tag{10}$$

Note that Δp is not simply proportional to the change in chemical potential $\Delta\mu = \lambda_v^2 n_v$ because of the non-ideality of the vapour and non-zero compressibility of the liquid in this model.

In the droplet case, the profile is found by solving equation (4). Since $\mu(n)$ is a linear function of n this can be done analytically in each of the three regions $0 \leqslant r \leqslant r_b$, $r_b \leqslant r \leqslant r_a$, and $r_a \leqslant r$, where r_a and r_b are defined implicitly by $n(r_a) = n_a$ and $n(r_b) = n_b$. Equations for r_a and r_b can be found by equating values of n and $\mathrm{d}n/\mathrm{d}r$ in adjacent regions at r_a and r_b and using the boundary conditions $\mathrm{d}n/\mathrm{d}r = 0$ at $r = 0$ and $n \to n_v$ as $r \to \infty$. This procedure yields

$$r_b \cos\Delta R + g(r_b)\sin\Delta R = r_a\left(1 - \frac{\lambda_2^2[n_b - n_a]}{\mu^*}\right) \tag{11}$$

$$r_b \sin \Delta R - g(r_b) \cos \Delta R = \frac{\lambda_2}{\mu^*}\left[\lambda_v r_a (n_a - n_v) + (n_b - n_v)\right] - \frac{1}{\lambda_2} \tag{12}$$

where $\Delta R = \lambda_2(r_a - r_b)$, $\mu^* = n_v\lambda_v^2 + (1 - n_b)\lambda_l^2$ and

$$g(r_b) = \frac{\lambda_2}{\lambda_l^2} - \frac{\lambda_2}{\lambda_l} r_b \coth \lambda_l r_b + \frac{1}{\lambda_2}. \tag{13}$$

Once suitable parameters are specified, equations (11) and (12) can be solved numerically for r_a and r_b. The density profile $n(r)$ is now completely specified and can be used in equation (3) to find $\Delta\Omega$. All of the integrations can be performed analytically, but the resulting somewhat lengthy expressions will not be reproduced here.

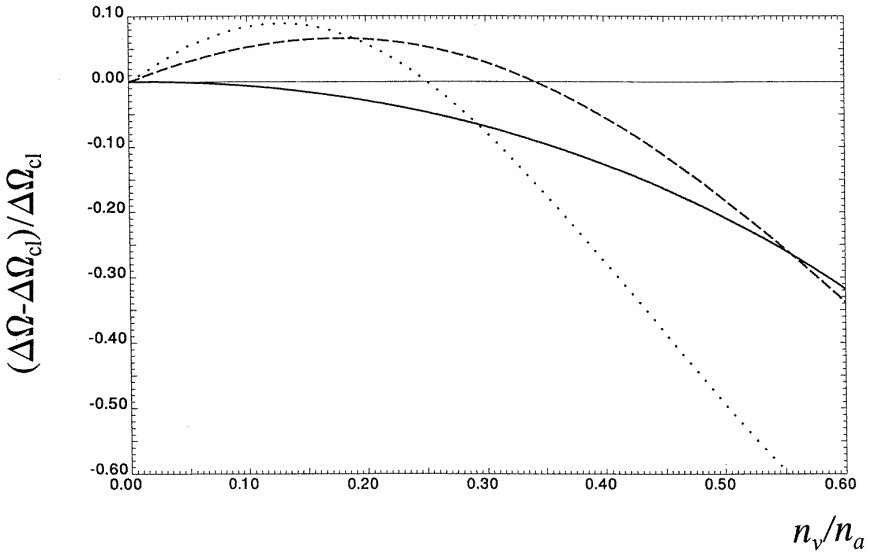

Figure 5. The variation of the fractional difference $[\Delta\Omega - \Delta\Omega_{Cl}]/\Delta\Omega_{Cl}$ with n_v/n_a for $\lambda_2/\lambda_v = 0.1$ (solid line), 1 (dashed line), and 10 (dotted line).

We are particularly interested in the sensitivity of the results to λ_2. Figure 5 shows the variation of the fractional difference $[\Delta\Omega - \Delta\Omega_{Cl}]/\Delta\Omega_{Cl}$ with n_v/n_a for $\lambda_l/\lambda_v = 0.7$ and three values of λ_2/λ_v. The ratio is positive for small values of n_v/n_a and negative for larger values, in agreement with Iwamatsu's results (which correspond to $\lambda_2 \to \infty$ in our model). Note that n_a depends on λ_2/λ_v according to equations (8) and (9): for $\lambda_2/\lambda_v = 0.1, 1, 10$ we have $n_a \approx 0.049$, 0.22, 0.41 respectively, so the curves in figure 5 correspond to very different values of n_v. Figure 6 shows the variation of the fractional difference with n_v for two values of λ_2/λ_v differing by 10%. These parameter values are comparable to those used in the semi-empirical treatment of nonane, but the sensitivity of the model to all parameter values makes it difficult to make even qualitative comparisons with real fluids. Nevertheless, figures 5 and 6 strongly suggest that results for real fluids will be sensitive to the form of the *p–n* curve in the unstable region.

We have shown that density gradient theory with scaled parameters fails to reproduce the results of mean-field density functional theory, and furthermore the results are sensitive to the form of the equation of state used, particularly in the experimentally inaccessible region between the two spinodals. These findings suggest that improvements to the

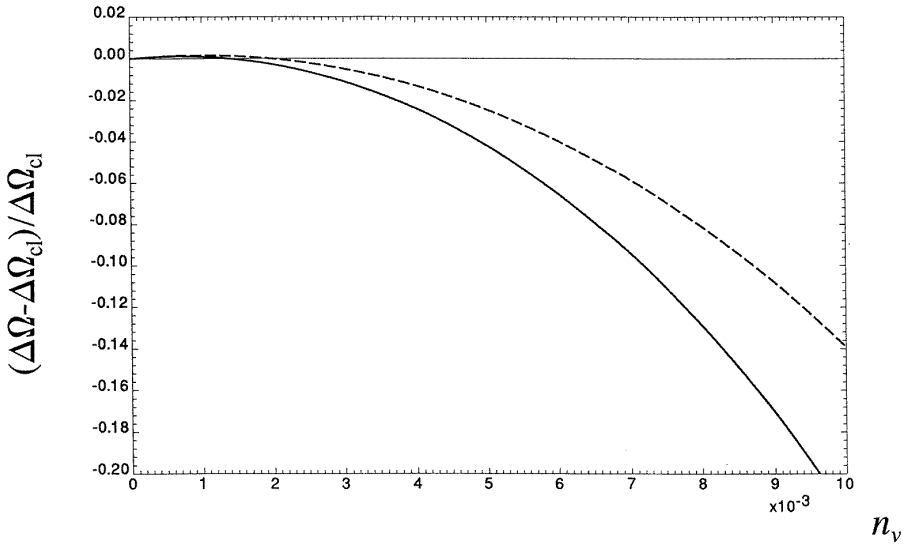

Figure 6. The variation of the fractional difference $[\Delta\Omega - \Delta\Omega_{Cl}]/\Delta\Omega_{Cl}$ with n_v for $\lambda_2/\lambda_v = 0.20$ (solid line) and 0.22 (dashed line).

density functional formalism for nucleation are needed before quantitative agreement with experiment can be expected. To date, work has concentrated on the hard-sphere part of the free-energy functional (see [13] for a review of recent advances), but these theories still reduce to the van der Waals form when a uniform density is assumed. Other improvements (such as an alternative division between core and attractive potential or an improved treatment of the attractive part of the functional) are likely to be required for a reliable density functional theory of nucleation. Comparisons with Monte Carlo results for model fluids, such as that performed by Lee *et al* [14], could also be useful in identifying the strengths and weaknesses of the density functional approach.

References

[1] Oxtoby D W and Evans R 1988 *J. Chem. Phys.* **89** 7521
[2] Zeng X C and Oxtoby D W 1991 *J. Chem. Phys.* **94** 4472
[3] Nyquist R M, Talanquer V and Oxtoby D W 1995 *J. Chem. Phys.* **103** 1175
[4] Barrett J C 1994 *Aerosols: Their Generation, Behaviour and Applications; Proc. 8th Annual Conf. of the Aerosol Society (York)* (Bristol: The Aerosol Society)
[5] Peng D Y and Robinson D B 1976 *Indust. Eng. Chem. Fundam.* **15** 59
[6] Oxtoby D W 1992 *J. Phys.: Condens. Matter* **4** 7627
[7] Evans R 1979 *Adv. Phys.* **28** 143
[8] Carey B S, Scriven L E and Davis H T 1978 *AIChE J.* **24** 1076
[9] Carnahan N F and Starling K E 1969 *J. Chem. Phys.* **51** 635
[10] Hung C, Krasnopoler M J and Katz J L 1989 *J. Chem. Phys.* **90** 1856
[11] Lu B Q, Evans R and Telo da Gama M M 1985 *Mol. Phys.* **55** 1319
[12] Iwamatsu M 1993 *J. Phys.: Condens. Matter* **5** 7537
[13] Evans R 1992 *Fundamentals of Inhomogeneous Fluids* ed D Henderson (New York: Dekker) ch 3
[14] Lee J K, Barker J A and Abraham F F 1974 *J. Chem. Phys.* **60** 246